

# Water-Induced Reversal of the TiO<sub>2</sub>(011)-(2 × 1) Surface Reconstruction: Observed with in Situ Surface X-ray Diffraction

Hadeel Hussain,<sup>†,‡</sup> Mahmoud H. M. Ahmed,<sup>†,‡</sup> Xavier Torrelles,<sup>§</sup> David C. Grinter,<sup>||</sup> Gregory Cabailh,<sup>⊥</sup> Oier Bikondoa,<sup>#,¶</sup> Christopher Nicklin,<sup>∇</sup> Ulrich Aschauer,<sup>○</sup> Robert Lindsay,<sup>†,‡</sup> and Geoff Thornton<sup>\*,||</sup>

<sup>†</sup>Corrosion and Protection Centre, School of Materials, The University of Manchester, Sackville Street, M13 9PL Manchester, U.K.

<sup>‡</sup>Photon Science Institute, The University of Manchester, M13 9PL Manchester, U.K.

<sup>§</sup>Institut de Ciència de Materials de Barcelona (CSIC), Campus UAB, 08193 Bellaterra, Spain

<sup>||</sup>London Centre for Nanotechnology and Department of Chemistry, University College London, 20 Gordon Street, WC1H 0AJ London, U.K.

<sup>⊥</sup>Sorbonne Université, UMR CNRS 7588, Institut des NanoSciences de Paris, 4 place Jussieu, 75252 Paris Cedex 05, France

<sup>#</sup>XMaS, The UK-CRG Beamline. ESRF, The European Synchrotron, 71, Avenue des Martyrs, CS40220, F-38043 Grenoble cedex 09, France

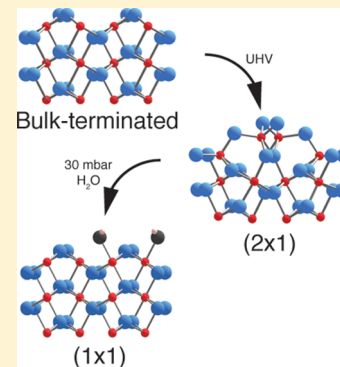
<sup>¶</sup>Department of Physics, University of Warwick, Gibbet Hill Road, CV4 7AL Coventry, U.K.

<sup>∇</sup>Diamond Light Source Limited, Diamond House, Harwell Science and Innovation Campus, Didcot, Oxfordshire OX11 0DE, U.K.

<sup>○</sup>Department of Chemistry and Biochemistry, University of Bern, Freiestrasse 3, 3012 Bern, Switzerland

## Supporting Information

**ABSTRACT:** The (011) termination of rutile TiO<sub>2</sub> is reported to be particularly effective for photocatalysis. Here, the structure of the interface formed between this substrate and water is revealed using surface X-ray diffraction. While the TiO<sub>2</sub>(011) surface exhibits a (2 × 1) reconstruction in ultra-high vacuum (UHV), this is lifted in the presence of a multilayer of water at room temperature. This change is driven by the formation of Ti–OH at the interface, which has a bond distance of 1.93 ± 0.02 Å. The experimental solution is in good agreement with density functional theory and first-principles molecular dynamics calculations. These results point to the important differences that can arise between the structure of oxide surfaces in UHV and technical environments and will ultimately lead to an atomistic understanding of the photocatalytic process of water splitting on TiO<sub>2</sub> surfaces.



## INTRODUCTION

Understanding the interaction of water on solid surfaces is of both fundamental and practical interest. Because many materials oxidize in ambient conditions, metal oxide studies are particularly pertinent for applications. Titanium dioxide, in particular the rutile (110) surface termination, has emerged as the prototypical metal oxide surface for fundamental studies.<sup>1</sup> After considerable effort, water adsorption on reduced rutile (110) surfaces is reasonably well understood: water dissociates at oxygen vacancies as well as <111> oriented steps at room temperature.<sup>1–5</sup> Terminal hydroxyls are reported to form at the interface with liquid water without reconstruction of the substrate,<sup>6</sup> although a recent paper has reported the role of carboxylates in the contact layer.<sup>7</sup> Whether water dissociates on the oxidized, stoichiometric surface remains a contentious issue.<sup>8–10</sup>

In this letter, we focus on the interface formed between water and the reportedly more photocatalytically active rutile-

TiO<sub>2</sub>(011) surface. We have previously determined the quantitative structure of the clean substrate, which exhibits a (2 × 1) reconstruction, in ultra-high vacuum (UHV) by means of surface X-ray diffraction (SXRD),<sup>11</sup> revealing a saw-tooth-like morphology with fivefold coordinated titanium atoms and twofold coordinated surface oxygen atoms arranged in rows along the [011] direction (Figure 1a). This structure has since been corroborated by other quantitative structural studies,<sup>12,13</sup> as well as density functional theory (DFT) calculations.<sup>14</sup>

As for water adsorption on TiO<sub>2</sub>(011)-(2 × 1), this has been investigated with ex situ scanning tunneling microscopy (STM). The results show that quasi-one-dimensional clusters populate the surface after exposure to 10<sup>-3</sup> Torr of water at room temperature.<sup>15</sup> Repeated scans led to partial removal of

Received: May 8, 2019

Revised: May 12, 2019

Published: May 13, 2019

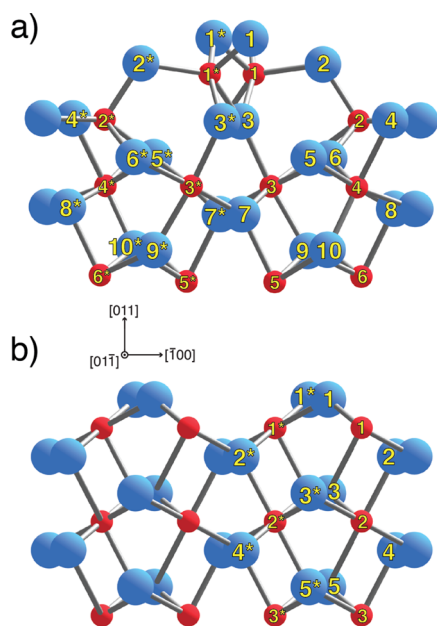


**Figure 1.** Ball and stick models of (a) the optimum  $\text{TiO}_2(011)-(2 \times 1)$  geometry and (b) the ideal bulk terminated  $\text{TiO}_2(011)$  structure. Large light blue (small red) spheres are oxygen (titanium) atoms. The numerical labeling of the atoms is employed in Tables 1 and S1 for the identification purposes. Symmetry paired atoms are denoted by an asterisk (\*).

these clusters, revealing a modified morphology. A first-principles molecular dynamics (FPMD) investigation<sup>16</sup> provides some insight as to what the structure may be. It suggests that there is a significant rearrangement of surface atoms upon exposure to  $\text{H}_2\text{O}$ , whereby the  $(2 \times 1)$  reconstruction reverts to a  $(1 \times 1)$  termination. It was also concluded that water dissociates at the interface to form a mixed molecular and dissociated overlayer (on average 3:1  $\text{H}_2\text{O}/\text{OH}$ ) at saturation coverage, with adsorption at surface Ti sites ( $\text{Ti}_{5c}$ ). More recently, a room-temperature STM experiment investigated the effect of dipping  $\text{TiO}_2(011)$  into liquid water.<sup>17</sup> This ex situ experiment identified a  $c(2 \times 1)$  half monolayer overlayer of OH by comparison with DFT calculations, with removal of the underlying  $(2 \times 1)$  reconstruction. Here, we employ SXRD to provide the first quantitative structure determination of the  $\text{TiO}_2(011)/\text{water}$  interface, performing in situ data acquisition at room temperature with an approximate  $\text{H}_2\text{O}$  coverage of 12 monolayers.

## EXPERIMENTAL AND THEORETICAL METHODS

Experimental work was performed at the Diamond Light Source, employing the Surface Village's off-line UHV chamber for sample preparation and beam line I07 for SXRD measurements.<sup>18</sup> In situ preparation of rutile  $\text{TiO}_2(011)$  involved repeated cycles of  $\text{Ar}^+$  bombardment and annealing in vacuum to  $\sim 1150$  K. A clean, well-ordered single-phase  $(2 \times 1)$  termination was achieved, in agreement with previous studies.<sup>11,13,19</sup> This was determined using low energy electron diffraction, X-ray photoelectron spectroscopy, and STM.

Once prepared, the sample was transferred under vacuum using a custom-built vacuum suitcase and UHV baby chamber combination (base pressure  $\sim 1.5 \times 10^{-9}$  mbar) incorporating a dome-shaped X-ray-transparent beryllium window suitable

for the collection of SXRD data. The chamber was mounted to I07's diffractometer, where data were collected using a 2D Pilatus photon detector. Measurements were carried out at room temperature with an incidence angle of  $1^\circ$  and a photon energy of 17.7 keV ( $=0.7$  Å). The sample was mounted such that the surface was in the horizontal plane. A systematic series of X-ray reflections were acquired in a stationary geometry ( $l$ -scans), that is, a full profile, including the background, is measured without scanning. For selected  $(h, k)$ , the intensity profile at regular intervals of  $l$ -values is measured. The spot intensity distribution on the 2D detector of the measured reflection is then integrated and corrected,<sup>20</sup> enabling profiles of scattered intensity versus perpendicular momentum transfer for both crystal truncation rods (CTRs) and fractional order rods (FORs). A reference reflection,  $(-1, 0, 0.97)$ , was recorded for both the clean and water covered surfaces at regular intervals to monitor surface degradation. No significant changes were observed throughout the duration of the experiment.

A sizeable dataset was taken for the UHV prepared sample [ $\text{TiO}_2(011)-(2 \times 1)$ ], comprising 10 419 reflections from 21 CTRs and 23 FORs that after averaging, using  $pg$  symmetry, were reduced to 5991 non-equivalent reflections. Subsequent to this, the chamber pump was switched off and the sample was exposed to a static pressure of  $\sim 30$  mbar of ultra-pure  $\text{H}_2\text{O}$  via back filling of the chamber, which equates to about twelve monolayers.<sup>21</sup> The chamber pump remained switched off for the duration of measurements. A further 4978 reflections from 22 CTRs were measured from this surface that reduced to 3507 non-equivalent reflections after averaging by the same symmetry. Water was thoroughly degassed using several freeze–pump–thaw cycles, with cleanliness confirmed by mass spectrometry (MKS Microvision Plus). Here, the partial pressure of water was increased to  $\sim 10$  mbar in the baby chamber and, through a precision leak valve, the differentially pumped mass spectrometer was exposed to a maximum of  $\sim 1 \times 10^{-6}$  mbar  $\text{H}_2\text{O}$ . Several masses were recorded simultaneously ( $\text{O} = 16$ ,  $\text{H}_2\text{O} = 18$ ,  $\text{CO} = 28$ ,  $\text{O}_2 = 32$ ,  $\text{CO}_2 = 44$ ,  $\text{CH}_2\text{O}_2 = 29, 46$  and  $\text{CH}_3\text{COOH} = 43, 45, 60$ ). While there was an increase of CO and  $\text{CO}_2$  to  $\sim 1 \times 10^{-8}$  mbar and  $\sim 5 \times 10^{-9}$  mbar, respectively, there was no indication of formic or acetic acid evolution.

The measured data were indexed with reference to a monoclinic unit cell defined by lattice vectors  $(a_1, a_2, a_3)$ . Lattice vectors  $a_1$  and  $a_2$  are directed along the  $[100]$  and  $[01\bar{1}]$  directions, respectively, and  $a_3$  lies in the plane defined by the  $[01\bar{1}]$  and  $[011]$  directions at an angle of  $\theta = 2 \times [\tan^{-1}(a/c)]$  with respect to  $a_2$ . The magnitudes of these lattice vectors are  $a_1 = 2 \times a$  and  $a_2 = a_3 = \sqrt{(a^2 + c^2)}$ , where  $a = 4.593$  Å and  $c = 2.958$  Å are the lattice constants of the tetragonal rutile  $\text{TiO}_2$  bulk unit cell.<sup>22</sup> Such a unit cell, rather than an orthorhombic unit cell with  $a_1, a_2,$  and  $a_3$  (all orthogonal to one another), was employed for structure determination in order to minimize the number of parameters varied during refinement. Corresponding reciprocal lattice vectors are denoted by  $h, k,$  and  $l$ . The best-fit analysis of the SXRD data recorded from  $\text{TiO}_2(011)-(2 \times 1)$  in UHV is shown in Figure S1. There is generally good agreement between the current optimum structure and that emerging from our previous study of this surface,<sup>11</sup> as demonstrated in Table S1.

For surface structure elucidation, the usual approach was adopted whereby theoretical SXRD data for a potential structure are generated. The structure is then iteratively refined to determine the best fit between experiment and theory. A modified version of the ROD software<sup>23</sup> was used for this task, in which the goodness-of-fit is measured by reduced  $\chi^2$ .<sup>24</sup>

Our DFT calculations were performed using the Quantum ESPRESSO package.<sup>25</sup> Main results were obtained using the Perdew–Burke–Ernzerhof (PBE) gradient corrected functional,<sup>26</sup> while additional calculations were performed using the DFT +  $U$  methodology<sup>27</sup> using a  $U$  value of 3.5 eV, which is in the range of values typically used for TiO<sub>2</sub>.<sup>28–30</sup> Wavefunctions were expanded in planewaves up to a kinetic energy of 25 Ry together with a cutoff of 200 Ry for the augmented density. We used ultrasoft<sup>31</sup> pseudopotentials with Ti(3s, 3p, 3d, 4s), O(2s, 2p), and H(1s) shells treated as valence electrons and modeled the unreconstructed rutile (011) surface using a 9.213 Å × 10.922 Å (2 × 2) surface supercell using the gamma point only for reciprocal space integration. Our slab model contained 4 TiO<sub>2</sub> tri-layers for a total thickness of 9.07 Å and a vacuum gap of 10.96 Å. For all calculations, the atoms in the bottom-most trilayer were kept fixed at their bulk positions. All other coordinates were relaxed until forces converged below 0.05 eV/Å. Water/OH was adsorbed at monolayer coverage on all under-coordinated Ti<sub>5c</sub> sites on the surface.

## RESULTS AND DISCUSSION

A comparison between three experimental CTRs for the clean surface and water covered interface of TiO<sub>2</sub>(011) is shown in Figure 2. The black and blue error bars represent the experimental data for the TiO<sub>2</sub>(011)-(2 × 1) and TiO<sub>2</sub>(011)/H<sub>2</sub>O surfaces, respectively. For ease of comparison, the CTRs for both data sets have been indexed with reference to the (1 × 1) bulk unit cell. Clear qualitative differences can be seen, particularly in the anti-Bragg regions of the [1,1,1] and [-4,0,1] CTRs (as indicated with red lines),

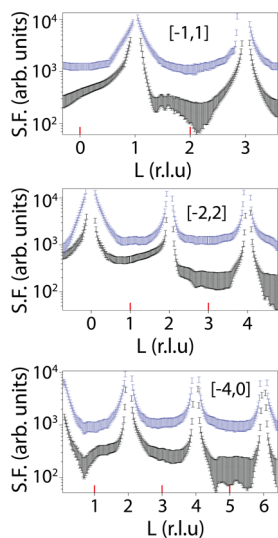


**Figure 2.** Comparison of experimental CTRs for TiO<sub>2</sub>(011)-(2 × 1) (bottom curve, black error bars) and TiO<sub>2</sub>(011)/H<sub>2</sub>O (top curve, blue error bars), respectively. Both are indexed using the same (1 × 1) unit cell for ease of comparison. For data analysis, the TiO<sub>2</sub>(011)-(2 × 1) dataset was re-indexed as (2\*H,K). CTRs are offset for clarity. Red lines on X-axis indicate the anti-Bragg regions.

where the asymmetrical line shape is no longer present after exposure to H<sub>2</sub>O, suggesting more bulk-like relaxation of the surface layers. Furthermore, the FOR intensity, which was observed for TiO<sub>2</sub>(011)-(2 × 1), is not present for TiO<sub>2</sub>(011)/H<sub>2</sub>O. This can be construed as a complete absence of the substrate reconstruction (i.e., that it is lifted in the presence of water) or that the domain size has reduced sufficiently to render the intensity of the FORs to background levels. To rigorously test for the presence of (2 × 1) reconstructed domains, refinement of atomic coordinates along with various nonstructural parameters of a model similar to the optimized TiO<sub>2</sub>(011)-(2 × 1) structure was undertaken.

By including an occupancy parameter to quantify the surface coverage of the (2 × 1) reconstruction, the model can determine if there is a “mixed” (2 × 1) reconstruction, in which both (1 × 1) and (2 × 1) domains exist or that there is a complete removal of the (2 × 1) termination. It was found during the fitting procedure that the occupancy of the (2 × 1) domains tended to a value close to zero, that is, the  $\chi^2$  reduces as the surface coverage of the (2 × 1) reconstruction reduces. This indicates that the presence of water induces more than just relaxations of substrate atoms at the interface and points to a model in which the substrate exhibits a bulk-like (1 × 1) termination. This is consistent with both theoretical (DFT) and experimental (STM) studies that have suggested a phase transition from (2 × 1) to (1 × 1) in the presence of water.<sup>16,17</sup> These studies concluded that the surface is decorated with OH/H<sub>2</sub>O tightly bound at all under-coordinated Ti<sub>5c</sub> sites in the presence of an aqueous environment,<sup>16</sup> while the surface adopts a configuration in which every second Ti<sub>5c</sub> row carries an OH when imaged in vacuum after exposure to liquid water.<sup>17</sup>

First, we consider the structural model resulting from DFT +  $U$  calculations in this work (see Table S2) for hydroxyls bound to every Ti<sub>5c</sub> site. The best  $\chi^2$  achieved (4.10) suggests poor agreement between experiment and this structure. This was found to be due to the relatively large atomic relaxations of Ti(1) and Ti(2) induced by the adsorption of OH forming “tight” bonds with Ti<sub>5c</sub> sites, when a monolayer coverage is assumed. When considering a model in which alternate Ti<sub>5c</sub> sites are occupied<sup>17</sup> where the large displacements of surface titanium atoms are suppressed (Figure 3), a  $\chi^2$  of 0.83 is

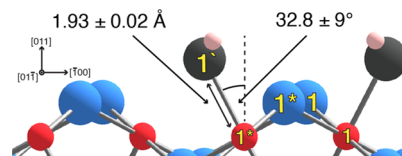


**Figure 3.** Ball and stick model of the local OH geometry for the optimized TiO<sub>2</sub>(011)/H<sub>2</sub>O substrate, indicating values for the bond angle and distance from best-fit structural parameters derived from SXRD. The atom color scheme and labels are the same as Figure 1. The large black atoms are oxygen atoms associated with OH.

achieved, which is indicative of excellent agreement between the experimental and calculated data (Figure S2). A total of 93 parameters were optimized during the structure refinement process, incorporating 78 atomic displacements, 10 Debye Waller (DW) factors, a scale factor, a surface roughness parameter, a surface fraction parameter, and 2 occupancy parameters—one for the (2 × 1) reconstructed domain and one for the adsorbate. The surface fraction parameter

confirmed that the entire surface adopts the structure obtained in this analysis. The optimum roughness parameter was  $\beta = 0.15$ , increasing from  $\beta = 0.09$  for the  $\text{TiO}_2(011)-(2 \times 1)$  structure. This is believed to be due to a combination of the change in the substrate termination and a manifestation of the dynamic nature of the water overlayer.<sup>16,32</sup> It should be noted that the presence of ordered water molecules in contact with the substrate or above the OH contact layer was tested for during data analysis. However, unlike the (110) surface of titania,<sup>6,33</sup> the occupancies of such molecules always tended toward zero, suggesting that water layers are completely disordered.

Based on this best-fit model, adsorbate ( $\text{O}(1')$ ) molecules preferentially adsorb to surface  $\text{Ti}_{5c}$  sites similar to that derived from STM and DFT +  $U$  calculations.<sup>16,17</sup> Removal of  $\text{O}(1')$  from our model increases the  $\chi^2$  to 1.1 (i.e., Figure 1b), indicating that the quality of the fit is sensitive to the presence of this adsorbate. As mentioned above, there are two unresolved questions in the literature regarding this adsorbate-decorated surface in an aqueous environment: (i) whether adsorption is mixed or fully dissociated and (ii) if the surface coverage is full or half monolayer. With regard to issue (i), the chemical identity of  $\text{O}(1')$  and thus confirmation of our best-fit model can be distinguished with SXR D by the length of the  $\text{Ti}-\text{O}(1')$  bond.

Figure 3 depicts the local adsorption geometry of atom  $\text{O}(1')$ , indicating values for the bond angle and distance from best-fit structural parameters derived from SXR D. A  $\text{Ti}-\text{O}(1')$  bond distance of  $1.93 \pm 0.02 \text{ \AA}$  is obtained in the current study, which agrees well with the DFT-calculated bond length at the PBE level of theory ( $1.87 \text{ \AA}$ ) and the  $\text{Ti}-\text{OH}$  bond length ( $1.95 \pm 0.03 \text{ \AA}$ ) found in a recent investigation of the interface formed between anatase  $\text{TiO}_2$  (101) and  $\text{H}_2\text{O}$ <sup>34</sup> as well as the  $\text{TiO}_2(110)/\text{water}$  interface.<sup>6</sup> PBE DFT calculations suggest a length of  $2.24 \text{ \AA}$  for the  $\text{Ti}-\text{H}_2\text{O}$  bond. This suggests that the contact layer consists of OH only rather than a mixed dissociated/molecular overlayer.

As a check to better define the chemical nature of  $\text{O}(1')$ , the  $\text{Ti}-\text{O}(1')$  bond distance was fixed at values indicative of  $\text{Ti}-\text{OH}$  bond distances ( $1.85 \text{ \AA}$ ) up to values typically associated with the  $\text{Ti}-\text{H}_2\text{O}$  bond distance ( $2.25 \text{ \AA}$ ) at intervals of  $0.05 \text{ \AA}$ , and the structure was optimized. This analysis in Figure S3 shows that varying the bond distance from  $1.85$  to  $2.25 \text{ \AA}$  results in a  $\Delta\chi^2$  of  $0.1$ , providing further evidence that the contact layer contains only OH (i.e.,  $1.93 \text{ \AA}$ ). All other bond distance values can be ruled out based on the uncertainty of the  $\chi^2$  ( $1/(N-p) = 0.0003$ ), as described elsewhere.<sup>32,35</sup> With regard to issue (ii), our best-fit structure derived from SXR D reveals an occupancy of  $0.5 \pm 0.02$  for  $\text{O}(1')$ , that is, half monolayer coverage of OH, in agreement with ref 17. Similar to issue (i), to better define this value, the occupancy of  $\text{O}(1')$  was varied at intervals of  $0.1$  ranging from no occupancy (0) to full occupancy (1), and the structure was optimized. The lowest  $\chi^2$  is achieved at an occupancy of  $0.5$  (Figure S4). All other occupancy values can be ruled out because of the small  $\chi^2$  uncertainty. In contrast to the full monolayer mixed  $\text{H}_2\text{O}/\text{OH}$  structure found in FPMD calculations,<sup>16</sup> the present experiments are best described by a half-monolayer of a purely OH structure. This difference could, besides the delicate and highly functional-dependent energetics of water dissociation, be related to the fact that in the FPMD calculations, the H fragment remained bound to the surface, enabling stabilization through H-bonding. This indicates that the precise adsorbate

coverage and structure of the surface could be sensitive to the pH of the aqueous phase, which affects the H coverage of the surface.

A question arises regarding the interaction between water molecules and the  $0.5 \text{ ML}$  of substrate not bound to OH. Insight can be garnered from recent ab initio molecular dynamics simulations on the adsorption of liquid water on the (110) surface of titania, where a similar  $(2 \times 1)\text{-OH}$  overlayer is formed.<sup>6</sup> Under aqueous conditions, the overlayer was found to be stabilized by diffusion of water molecules between the contact and multilayer such that the average occupation of  $\text{Ti}_{5c}$  sites adjacent to the adsorbed OH molecules is  $0.18 \text{ ML}$  over the total length of the simulation. It is likely that the same adsorption/desorption process of the water molecules occurs on the (011) termination. Although partial occupation of water on the substrate is not observed in the (011) and (110) SXR D data, this is expected, given the large associated DW factors and likely relatively low occupancy.

Table 1 lists the atomic positions, expressed as displacements from the bulk-terminated  $\text{TiO}_2(011)-(1 \times 1)$  surface, of

**Table 1. Optimized Atomic Displacements of the  $\text{TiO}_2(011)/\text{H}_2\text{O}$  and  $\text{TiO}_2(011)-(2 \times 1)$  Structures Resulting from Analysis of SXR D Data**

| atom <sup>a</sup> | displacements ( $\text{\AA}$ )           |  |  |
|-------------------|--|--|--|
|                   | $\Delta x$ [ $\text{H}_2\text{O}$ : UHV] | $\Delta y$ [ $\text{H}_2\text{O}$ : UHV] | $\Delta z$ [ $\text{H}_2\text{O}$ : UHV] |
| $\text{O}(1')$    | N/A                                      | N/A                                      | N/A                                      |
| $\text{O}(1)$     | $0.05 \pm 0.02$                          | $0.02 \pm 0.03$                          | $0.16 \pm 0.02$                          |
| $\text{Ti}(1)$    | $-2.48 \pm 0.02$                         | $2.91 \pm 0.03$                          | $0.59 \pm 0.03$                          |
| $\text{O}(2)$     | $0.03 \pm 0.01$                          | $0.00 \pm 0.01$                          | $0.01 \pm 0.01$                          |
| $\text{O}(3)$     | $-0.56 \pm 0.01$                         | $0.32 \pm 0.01$                          | $0.42 \pm 0.01$                          |
| $\text{Ti}(2)$    | $-0.01 \pm 0.02$                         | $-0.15 \pm 0.02$                         | $0.15 \pm 0.02$                          |
| $\text{O}(4)$     | $-0.12 \pm 0.02$                         | $-0.31 \pm 0.02$                         | $-0.06 \pm 0.03$                         |
| $\text{O}(5)$     | $-0.01 \pm 0.02$                         | $-0.09 \pm 0.02$                         | $-0.03 \pm 0.02$                         |
| $\text{Ti}(3)$    | $-0.05 \pm 0.01$                         | $0.27 \pm 0.03$                          | $-0.04 \pm 0.03$                         |
| $\text{O}(6)$     | $-0.04 \pm 0.01$                         | $-0.01 \pm 0.01$                         | $0.01 \pm 0.01$                          |
| $\text{O}(7)$     | $-0.08 \pm 0.01$                         | $-1.76 \pm 0.01$                         | $-0.77 \pm 0.01$                         |
| $\text{O}(8)$     | $0.02 \pm 0.02$                          | $-0.02 \pm 0.02$                         | $0.05 \pm 0.02$                          |
| $\text{O}(9)$     | $-0.11 \pm 0.01$                         | $0.43 \pm 0.03$                          | $0.01 \pm 0.03$                          |
| $\text{O}(10)$    | $0.02 \pm 0.02$                          | $-0.08 \pm 0.02$                         | $0.00 \pm 0.02$                          |
| $\text{O}(11)$    | $0.05 \pm 0.01$                          | $0.02 \pm 0.02$                          | $-0.08 \pm 0.02$                         |
| $\text{Ti}(4)$    | $-0.01 \pm 0.01$                         | $-0.01 \pm 0.01$                         | $0.01 \pm 0.01$                          |
| $\text{Ti}(5)$    | $-0.17 \pm 0.01$                         | $-0.03 \pm 0.01$                         | $-0.07 \pm 0.01$                         |

<sup>a</sup>Figures 1 and 3 provide a key to the identity of the atoms. A positive value for  $x$ ,  $y$ , and  $z$  indicates a displacement in the  $[100]$ ,  $[011]$ , and  $[011]$  directions, respectively.

the best-fit structures for  $\text{TiO}_2(011)-(2 \times 1)$  and  $\text{TiO}_2(011)/\text{H}_2\text{O}$  (atomic coordinates listed in Table 2). It can be clearly seen that after exposure to  $\text{H}_2\text{O}$  practically all atoms in the selvage appear to have bulk-like displacements, a phenomenon not uncommon to metal oxide surfaces.<sup>6,32,34,35</sup> This is especially the case for the surface layer [atoms  $\text{O}(1)$  and  $\text{Ti}(1)$ ] and explains why the asymmetrical line shape in the anti-Bragg regions of the CTRs for  $\text{TiO}_2(011)-(2 \times 1)$  are no longer present for  $\text{TiO}_2(011)/\text{H}_2\text{O}$  (Figures S1 and S2). Finally, to rule out adventitious formate (and carbonate) adsorption, which has been reported at the bulk water interface with  $\text{TiO}_2(110)$ ,<sup>7,36</sup> we carried out a trial fit of our data with formate/carbonate replacing OH as the adsorbate in a bidentate configuration to adjacent fivefold coordinated Ti

**Table 2. Optimized Atomic Coordinates of the TiO<sub>2</sub>(011)/H<sub>2</sub>O Structure Resulting from Analysis of SXRD Data**

| atom <sup>a</sup> | bulk terminated (x, y, z) coordinates (Å) | TiO <sub>2</sub> (011)/H <sub>2</sub> O (x, y, z) coordinates (Å) |
|-------------------|---|---|
| O(1')             | N/A                                       | -1.44, 3.41, 1.89   |
| O(1)              | 0.89, 1.90, 0.83                          | 0.94, 1.92, 0.99  |
| Ti(1)             | 0.00, 0.00, 0.00                          | 0.03, 0.00, 0.01  |
| O(2)              | -1.40, 0.83, -0.83                        | -1.41, 0.68, -0.68  |
| O(3)              | 1.40, 1.90, -1.90                         | 1.39, 1.81, -1.93   |
| Ti(2)             | 0.00, 2.73, -2.73                         | -0.04, 2.72, -2.72  |
| O(4)              | -1.40, 3.57, -3.56                        | -1.38, 3.55, -3.51  |
| O(5)              | 0.89, 1.90, -4.63                         | 0.91, 1.82, -4.63   |
| Ti(3)             | 0.00, 0.00, -5.46                         | -0.01, -0.01, -5.45   |

<sup>a</sup>Figures 1 and 3 provide a key to the identity of the atoms. A positive value for x, y, and z indicates a displacement in the [100], [011], and [011] directions, respectively.

sites. The best-fit  $\chi^2$  achieved was 1.30, an increase of 57% compared with that achieved with OH.

Finally, in comparison to previous work on the TiO<sub>2</sub>(011)/H<sub>2</sub>O system in UHV, we observe both similarities and differences.<sup>15,37,38</sup> Combined theoretical and experimental studies<sup>37,38</sup> concluded that molecular water adsorption is only possible at temperatures below 200 K, where a mixed dissociative overlayer is favored. At room temperature, a fully dissociated overlayer of submonolayer coverage exists. Reference 37 assumes the (2 × 1) reconstruction remains after water adsorption. An ex situ STM study<sup>15</sup> has shown that exposing the surface to approximately 10<sup>-3</sup> Torr H<sub>2</sub>O leads to a modified surface morphology and concluded that a full adsorption layer of water is necessary for the restructuring to be energetically favorable.

## CONCLUSIONS

In summary, we have used SXRD to determine the structure of the photocatalytically active TiO<sub>2</sub>(011)/water interface. Our results point to the formation of half-monolayer OH in the contact layer, which causes the substrate to revert to a bulk-like termination from the (2 × 1) reconstruction adopted in UHV. These results compare well with recent experimental and theoretical investigations in the literature and will aid efforts to provide an atomic scale understanding of the enhanced photocatalytic activity displayed by the TiO<sub>2</sub>(011) surface in aqueous environments.

## ASSOCIATED CONTENT

### Supporting Information

The Supporting Information is available free of charge on the ACS Publications website at DOI: 10.1021/acs.jpcc.9b04383.

Ball and stick model of the optimized TiO<sub>2</sub>(011)/H<sub>2</sub>O substrate obtained from DFT + U calculations for 1 ML OH coverage and ball and stick model of the optimized TiO<sub>2</sub>(011)/H<sub>2</sub>O substrate obtained from SXRD (CIF) Optimized atomic coordinates obtained from DFT + U calculations of TiO<sub>2</sub>(011)/H<sub>2</sub>O at 1 ML coverage of OH and optimized atomic coordinates obtained from SXRD data acquired from TiO<sub>2</sub>(011)/H<sub>2</sub>O (XYZ) Brief description of SXRD analysis for the TiO<sub>2</sub>(011)-(2 × 1) surface; FORs and CTRs from the optimized TiO<sub>2</sub>(011)-(2 × 1) surface; CTR data from the optimized TiO<sub>2</sub>(011)/water interface;  $\chi^2$  against Ti-O(1') bond distance from the optimized TiO<sub>2</sub>(011)/

water interface;  $\chi^2$  against O(1') occupancy from the optimized TiO<sub>2</sub>(011)/water interface; ; tabulated positional parameters from the best-fit model of the SXRD data from TiO<sub>2</sub>(011)-(2 × 1); and tabulated positional parameters from the best-fit model obtained from DFT + U calculations for TiO<sub>2</sub>(011)/water interface at 1 ML coverage (PDF)

## AUTHOR INFORMATION

### Corresponding Author

\*E-mail: g.thornton@ucl.ac.uk

### ORCID

Hadeel Hussain: 0000-0002-1322-261X

Xavier Torrelles: 0000-0002-6891-7793

Gregory Cabailh: 0000-0002-8053-2132

Oier Bikondoa: 0000-0001-9004-9032

Ulrich Aschauer: 0000-0002-1165-6377

Robert Lindsay: 0000-0001-5050-669X

Geoff Thornton: 0000-0002-1616-5606

### Notes

The authors declare no competing financial interest.

## ACKNOWLEDGMENTS

We thank Annabella Selloni for useful discussions. This work was supported by the European Research Council Advanced Grant ENERGYSURF (G.T.), EPSRC (UK) (EP/D068673/1), EU COST Action CM1104, the Royal Society (UK) through a Wolfson Research Merit Award to G.T., and M.E.C. (Spain) through project MAT2015-686760-C2-2-P, Severo Ochoa SEV-2015-0496 grant, and project EFA194/16/TNSI funded by interreg POCTEFA program. M.H.M.A. acknowledges financial support from EPSRC through the Advanced Metallic Systems Centre for Doctoral Training (EP/G036950/1) and from BP. H.H. would like to acknowledge funding from BP through the BP International Centre for Advanced Materials (BP-ICAM). U.A. was supported by the SNF Professorship grant PP00P2\_157615. Calculations were performed on UBELIX (<http://www.id.unibe.ch/hpc>), the HPC cluster at the University of Bern.

## REFERENCES

- (1) Pang, C. L.; Lindsay, R.; Thornton, G. Structure of Clean and Adsorbate-Covered Single-Crystal Rutile TiO<sub>2</sub> Surfaces. *Chem. Rev.* **2013**, *113*, 3887–3948.
- (2) Henderson, M. A. A Surface Science Perspective on TiO<sub>2</sub> Photocatalysis. *Surf. Sci. Rep.* **2011**, *66*, 185–297.
- (3) Brookes, I. M.; Muryn, C. A.; Thornton, G. Imaging Water Dissociation on TiO<sub>2</sub>(110). *Phys. Rev. Lett.* **2001**, *87*, 266103.
- (4) Bikondoa, O.; Pang, C. L.; Ithnin, R.; Muryn, C. A.; Onishi, H.; Thornton, G. Direct Visualization of Defect-Mediated Dissociation of Water on TiO<sub>2</sub>(110). *Nat. Mater.* **2006**, *5*, 189–192.
- (5) Kristoffersen, H. H.; Hansen, J. Ø.; Martinez, U.; Wei, Y. Y.; Matthiesen, J.; Streber, R.; Bechstein, R.; Lægsgaard, E.; Besenbacher, F.; Hammer, B.; et al. Role of Steps in the Dissociative Adsorption of Water on Rutile TiO<sub>2</sub>(110). *Phys. Rev. Lett.* **2013**, *110*, 146101.
- (6) Hussain, H.; Tocci, G.; Woolcot, T.; Torrelles, X.; Pang, C. L.; Humphrey, D. S.; Yim, C. M.; Grinter, D. C.; Cabailh, G.; Bikondoa, O.; et al. Structure of a Model TiO<sub>2</sub> Photocatalytic Interface. *Nat. Mater.* **2017**, *16*, 461–466.
- (7) Balajka, J.; Hines, M. A.; DeBenedetti, W. J. I.; Komora, M.; Pavelec, J.; Schmid, M.; Diebold, U. High-Affinity Adsorption Leads to Molecularly Ordered Interfaces on TiO<sub>2</sub> in Air and Solution. *Science* **2018**, *361*, 786–789.

- (8) Liu, L.-M.; Zhang, C.; Thornton, G.; Michaelides, A. Structure and Dynamics of Liquid Water on Rutile  $\text{TiO}_2(110)$ . *Phys. Rev. B: Condens. Matter Mater. Phys.* **2010**, *82*, 161415.
- (9) Raju, M.; Kim, S.-Y.; van Duin, A. C. T.; Fichthorn, K. A. ReaxFF Reactive Force Field Study of the Dissociation of Water on Titania Surfaces. *J. Phys. Chem. C* **2013**, *117*, 10558–10572.
- (10) Zhang, Z.; Fenter, P.; Sturchio, N. C.; Bedzyk, M. J.; Machesky, M. L.; Wesolowski, D. J. Structure of Rutile  $\text{TiO}_2(110)$  in Water and 1 Molal  $\text{Rb}^+$  at PH 12: Inter-Relationship among Surface Charge, Interfacial Hydration Structure, and Substrate Structural Displacements. *Surf. Sci.* **2007**, *601*, 1129–1143.
- (11) Torrelles, X.; Cabailh, G.; Lindsay, R.; Bikondoa, O.; Roy, J.; Zegenhagen, J.; Teobaldi, G.; Hofer, W. A.; Thornton, G. Geometric Structure of  $\text{TiO}_2(011)(2 \times 1)$ . *Phys. Rev. Lett.* **2008**, *101*, 185501.
- (12) Gong, X.-Q.; Khorshidi, N.; Stierle, A.; Vonk, V.; Ellinger, C.; Dosch, H.; Cheng, H.; Selloni, A.; He, Y.; Dulub, O.; et al. The  $2 \times 1$  Reconstruction of the Rutile  $\text{TiO}_2(011)$  Surface: A Combined Density Functional Theory, X-Ray Diffraction, and Scanning Tunneling Microscopy Study. *Surf. Sci.* **2009**, *603*, 138–144.
- (13) Chamberlin, S. E.; Hirschmugl, C. J.; Poon, H. C.; Saldin, D. K. Geometric Structure of  $(011)(2 \times 1)$  Surface by Low Energy Electron Diffraction (LEED). *Surf. Sci.* **2009**, *603*, 3367–3373.
- (14) Woolcot, T.; Teobaldi, G.; Pang, C. L.; Beglitis, N. S.; Fisher, A. J.; Hofer, W. A.; Thornton, G. Scanning Tunneling Microscopy Contrast Mechanisms for  $\text{TiO}_2$ . *Phys. Rev. Lett.* **2012**, *109*, 156105.
- (15) Cuan, Q.; Tao, J.; Gong, X.-Q.; Batzill, M. Adsorbate Induced Restructuring of  $\text{TiO}_2(011)-(2 \times 1)$  Leads to One-Dimensional Nanocluster Formation. *Phys. Rev. Lett.* **2012**, *108*, 106105.
- (16) Aschauer, U.; Selloni, A. Structure of the Rutile  $\text{TiO}_2(011)$  Surface in an Aqueous Environment. *Phys. Rev. Lett.* **2011**, *106*, 166102.
- (17) Balajka, J.; Aschauer, U.; Mertens, S. F. L.; Selloni, A.; Schmid, M.; Diebold, U. Surface Structure of  $\text{TiO}_2$  Rutile (011) Exposed to Liquid Water. *J. Phys. Chem. C* **2017**, *121*, 26424–26431.
- (18) Nicklin, C.; Arnold, T.; Rawle, J.; Warne, A. Diamond Beamline I07: A Beamline for Surface and Interface Diffraction. *J. Synchrotron Radiat.* **2016**, *23*, 1245–1253.
- (19) Dulub, O.; Valentin, C. D.; Selloni, A.; Diebold, U. Structure, Defects, and Impurities at the Rutile  $\text{TiO}_2(011)-(2 \times 1)$  Surface: A Scanning Tunneling Microscopy Study. *Surf. Sci.* **2006**, *600*, 4407–4417.
- (20) Vlieg, E. A  $(2+3)$ -Type Surface Diffractometer: Mergence of the z-Axis and  $(2+2)$ -Type Geometries. *J. Appl. Crystallogr.* **1998**, *31*, 198–203.
- (21) Ketteler, G.; Yamamoto, S.; Bluhm, H.; Andersson, K.; Starr, D. E.; Ogletree, D. F.; Ogasawara, H.; Nilsson, A.; Salmeron, M. The Nature of Water Nucleation Sites on  $\text{TiO}_2(110)$  Surfaces Revealed by Ambient Pressure X-Ray Photoelectron Spectroscopy. *J. Phys. Chem. C* **2007**, *111*, 8278–8282.
- (22) Wells, A. F. *Structural Inorganic Chemistry*; Wells, A. F., Ed.; Clarendon Press, 1985.
- (23) Vlieg, E. ROD: A Program for Surface X-Ray Crystallography. *J. Appl. Crystallogr.* **2000**, *33*, 401–405.
- (24) Feidenhans'l, R. Surface Structure Determination by X-Ray Diffraction. *Surf. Sci. Rep.* **1989**, *10*, 105–188.
- (25) Giannozzi, P.; Baroni, S.; Bonini, N.; Calandra, M.; Car, R.; Cavazzoni, C.; Ceresoli, D.; Chiarotti, G. L.; Cococcioni, M.; Dabo, I.; et al. QUANTUM ESPRESSO: A Modular and Open-Source Software Project for Quantum Simulations of Materials. *J. Phys.: Condens. Matter* **2009**, *21*, 395502.
- (26) Perdew, J. P.; Burke, K.; Ernzerhof, M. Generalized Gradient Approximation Made Simple. *Phys. Rev. Lett.* **1996**, *77*, 3865–3868.
- (27) Anisimov, V. I.; Zaanen, J.; Andersen, O. K. Band Theory and Mott Insulators: Hubbard  $U$  Instead of Stoner  $I$ . *Phys. Rev. B: Condens. Matter Mater. Phys.* **1991**, *44*, 943–954.
- (28) Cheng, H.; Selloni, A. Energetics and Diffusion of Intrinsic Surface and Subsurface Defects on Anatase  $\text{TiO}_2(101)$ . *J. Chem. Phys.* **2009**, *131*, 054703.
- (29) Finazzi, E.; Di Valentin, C.; Pacchioni, G.; Selloni, A. Excess Electron States in Reduced Bulk Anatase  $\text{TiO}_2$ : Comparison of Standard GGA, GGA+U, and Hybrid DFT Calculations. *J. Chem. Phys.* **2008**, *129*, 154113.
- (30) Mattioli, G.; Filippone, F.; Alippi, P.; Amore Bonapasta, A. Ab Initio Study of the Electronic States Induced by Oxygen Vacancies in Rutile and Anatase  $\text{TiO}_2$ . *Phys. Rev. B: Condens. Matter Mater. Phys.* **2008**, *78*, 241201.
- (31) Vanderbilt, D. Soft Self-Consistent Pseudopotentials in a Generalized Eigenvalue Formalism. *Phys. Rev. B: Condens. Matter Mater. Phys.* **1990**, *41*, 7892–7895.
- (32) Ahmed, M. H. M.; Torrelles, X.; Treacy, J. P. W.; Hussain, H.; Nicklin, C.; Wincott, P. L.; Vaughan, D. J.; Thornton, G.; Lindsay, R. Geometry of  $\alpha\text{-Cr}_2\text{O}_3(0001)$  as a Function of  $\text{H}_2\text{O}$  Partial Pressure. *J. Phys. Chem. C* **2015**, *119*, 21426–21433.
- (33) Treacy, J. P. W.; Hussain, H.; Torrelles, X.; Cabailh, G.; Bikondoa, O.; Nicklin, C.; Thornton, G.; Lindsay, R. Structure of a Superhydrophilic Surface: Wet Chemically Prepared Rutile- $\text{TiO}_2(110)(1 \times 1)$ . *J. Phys. Chem. C* **2019**, *123*, 8463–8468.
- (34) Nadeem, I. M.; Treacy, J. P. W.; Selcuk, S.; Torrelles, X.; Hussain, H.; Wilson, A.; Grinter, D. C.; Cabailh, G.; Bikondoa, O.; Nicklin, C.; et al. Water Dissociates at the Aqueous Interface with Reduced Anatase  $\text{TiO}_2(101)$ . *J. Phys. Chem. Lett.* **2018**, *9*, 3131–3136.
- (35) Hussain, H.; Torrelles, X.; Rajput, P.; Nicotra, M.; Thornton, G.; Zegenhagen, J. A Quantitative Structural Investigation of the 0.1 Wt % Nb– $\text{SrTiO}_3(001)/\text{H}_2\text{O}$  Interface. *J. Phys. Chem. C* **2014**, *118*, 10980–10988.
- (36) Song, A.; Skibinski, E. S.; DeBenedetti, W. J. I.; Ortoll-Bloch, A. G.; Hines, M. A. Nanoscale Solvation Leads to Spontaneous Formation of a Bicarbonate Monolayer on Rutile (110) under Ambient Conditions: Implications for  $\text{CO}_2$  Photoreduction. *J. Phys. Chem. C* **2016**, *120*, 9326–9333.
- (37) Beck, T. J.; Klust, A.; Batzill, M.; Diebold, U.; Di Valentin, C.; Tilocca, A.; Selloni, A. Mixed Dissociated/Molecular Monolayer of Water on the  $\text{TiO}_2(011)-(2 \times 1)$  Surface. *Surf. Sci.* **2005**, *591*, L267–L272.
- (38) Di Valentin, C.; Tilocca, A.; Selloni, A.; Beck, T. J.; Klust, A.; Batzill, M.; Losovyj, Y.; Diebold, U. Adsorption of Water on Reconstructed Rutile  $\text{TiO}_2(011)-(2 \times 1)$ :  $\text{TiO}$  Double Bonds and Surface Reactivity. *J. Am. Chem. Soc.* **2005**, *127*, 9895–9903.